

Evidence for a solar cycle influence on the infrared energy budget and radiative cooling of the thermosphere

Martin G. Mlynczak,¹ F. Javier Martin-Torres,² B. Thomas Marshall,³ R. Earl Thompson,³ Joshua Williams,⁴ Timothy Turpin,⁴ David P. Kratz,¹ James M. Russell III,⁵ Tom Woods,⁶ and Larry L. Gordley³

Received 27 November 2006; revised 10 August 2007; accepted 28 August 2007; published 6 December 2007.

[1] We present direct observational evidence for solar cycle influence on the infrared energy budget and radiative cooling of the thermosphere. By analyzing nearly five years of data from the Sounding of the Atmosphere using Broadband Emission Radiometry (SABER) instrument, we show that the annual mean infrared power radiated by the nitric oxide (NO) molecule at 5.3 μm has decreased by a factor of 2.9. This decrease is correlated ($r = 0.96$) with the decrease in the annual mean F10.7 solar index. Despite the sharp decrease in radiated power (which is equivalent to a decrease in the vertical integrated radiative cooling rate), the variability of the power as given in the standard deviation of the annual means remains approximately constant. A simple relationship is shown to exist between the infrared power radiated by NO and the F10.7 index, thus providing a fundamental relationship between solar activity and the thermospheric cooling rate for use in thermospheric models. The change in NO radiated power is also consistent with changes in absorbed ultraviolet radiation over the same time period. Computations of radiated power using an empirical model show much less variability than observed by SABER.

Citation: Mlynczak, M. G., F. J. Martin-Torres, B. T. Marshall, R. E. Thompson, J. Williams, T. Turpin, D. P. Kratz, J. M. Russell, III, T. Woods, and L. L. Gordley (2007), Evidence for a solar cycle influence on the infrared energy budget and radiative cooling of the thermosphere, *J. Geophys. Res.*, 112, A12302, doi:10.1029/2006JA012194.

1. Introduction

[2] The primary radiative cooling mechanism in the terrestrial thermosphere is the infrared emission from the NO molecule at 5.3 μm [Kockarts, 1980]. Although the emission has been measured previously during suborbital rocket flights and by the Improved Stratospheric and Mesospheric Sounder instrument on the Upper Atmosphere Research Satellite [Ballard *et al.*, 1993], long-term global observations of this fundamental process were not available until the launch of the NASA Thermosphere-Ionosphere-Mesosphere Energetics and Dynamics (TIMED) satellite in December 2001. The SABER instrument on the TIMED satellite continuously observes the NO 5.3- μm emission at high vertical and horizontal resolution, enabling global characterization of the radiative cooling and its variability. SABER records

approximately 1600 vertical profiles of NO limb radiance per day. Over 2.5 million radiance profiles (encompassing approximately 1 billion individual limb radiance samples) are used in this analysis. The results presented here are from version 1.06 of the SABER data set.

[3] Since the TIMED launch, a focus of the analyses of the SABER NO emission data has been on the “natural thermostat” effect of nitric oxide in response to intense geomagnetic storms caused by coronal mass ejections [Mlynczak *et al.*, 2003, 2005]. These analyses laid the groundwork for understanding the role infrared radiation plays in allowing the thermosphere to rapidly recover from perturbations caused by geomagnetic disturbances. In this paper we apply the same analysis techniques as in the work of Mlynczak *et al.* [2003, 2005], but to the entire SABER data set now nearing five years in length. The analysis reveals a remarkable decrease in radiated power from the thermosphere during this time, a decrease that is strongly correlated with the decrease in the solar 10.7 cm radio flux as indicated by the F10.7 index. This correlation strongly implies the decrease in radiated NO power is associated with the declining activity of the present solar cycle.

[4] In section 2 we review the analysis procedure used to derive the daily global radiated power from the measured SABER limb radiances. In section 3 we present the results of this analysis, on a year-by-year basis, including the running annual means. The results are discussed in section 3 wherein

¹NASA Langley Research Center, Hampton, Virginia, USA.

²Analytic Services & Materials, Inc., Hampton, Virginia, USA.

³G&A Technical Software, Newport News, Virginia, USA.

⁴Department of Electrical and Computer Engineering, Utah State University, Logan, Utah, USA.

⁵Center for Atmospheric Sciences, Hampton University, Hampton, Virginia, USA.

⁶Laboratory for Atmospheric and Space Physics, Boulder, Colorado, USA.

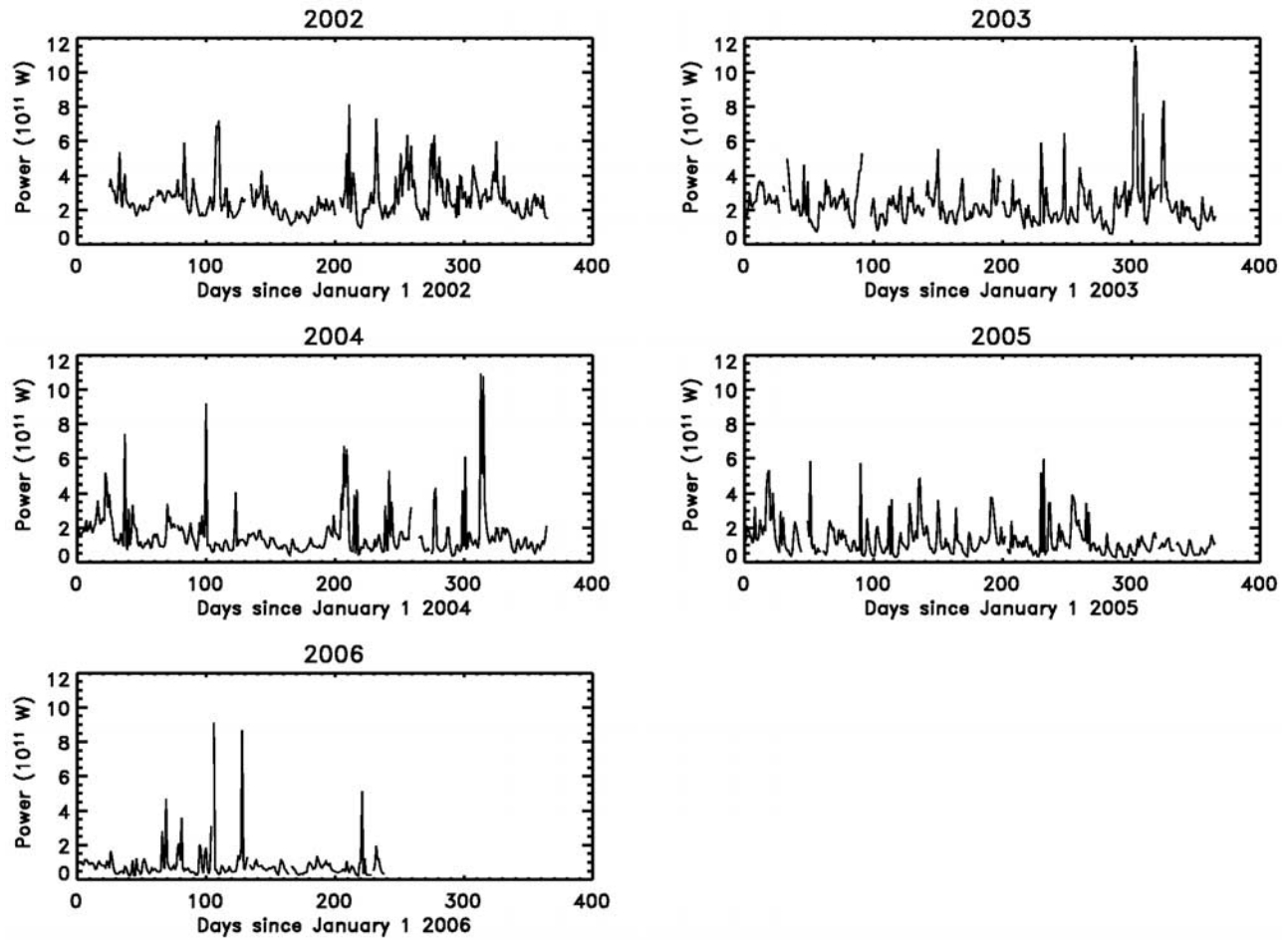


Figure 1. Daily global power (W) radiated by NO from 2002 to 2006.

simple relationship between the annual mean F10.7 index and the annual mean NO power is given. Analysis of the results is given in section 4, followed by a comparison with the solar input variability in section 5. A comparison of the observed power with that derived from an empirical model is given in section 6. The paper concludes with a summary section.

2. Analysis Technique

[5] In this paper we follow the analysis technique given in the work of *Mlynchak et al.* [2005]. For each day we derive the global power radiated by the NO molecule from SABER limb radiance measurements. The essential steps of this technique are reviewed here.

[6] First, an Abel inversion is applied to the SABER-measured limb radiance ($\text{W m}^{-2} \text{sr}^{-1}$) to yield a volume emission rate (W m^{-3}) of energy. The Abel inversion is valid because the radiative transfer is in the weak-line limit. However, because SABER is a filter radiometer, the volume emission rate derived in this step is not representative of the total rate of emission from the NO molecule. Rather, it is a measure of the total emission as weighted by the relative spectral response function of the SABER instrument. In order to account for the effect of the spectral filter and obtain the total (unweighted) emission from the NO mole-

cule, an “unfilter” correction factor, presently derived from theory, is computed at each altitude. The unfilter factor is the ratio of the total radiative emission from the NO molecule to the in-band radiative emission. The unweighted SABER emission is derived by multiplying the retrieved in-band emission rate by the unfilter factor. The factor is different for day and night and ranges from approximately 2.25 at 100 km to nearly 3.6 at 200 km. Stated differently, at 100 km approximately 44% ($1.0/2.25$) of the NO emission falls within the SABER band pass, while at 200 km only 28% ($1.0/3.6$) of the emission is within the band pass. We note that *Gardner et al.* [2007] have independently derived the unfilter factor by analyzing NO spectra recorded by the MIPAS instrument on the Envisat satellite. Their analysis confirms the theoretical values used in the operational SABER data processing.

[7] The next step after deriving the total NO emission rate in W m^{-3} is to vertically integrate this rate to obtain the flux (W m^{-2}) of energy out of the thermosphere. All of the radiation emitted by NO escapes the thermosphere; one-half of it exits to space, the other is absorbed in the lower atmosphere. The radiation absorbed in the lower atmosphere is not a significant source of heat there. The emission is absorbed over a range of altitudes where the density is substantially higher than where it originates in the thermosphere. So while in fact the downwelling NO emission is

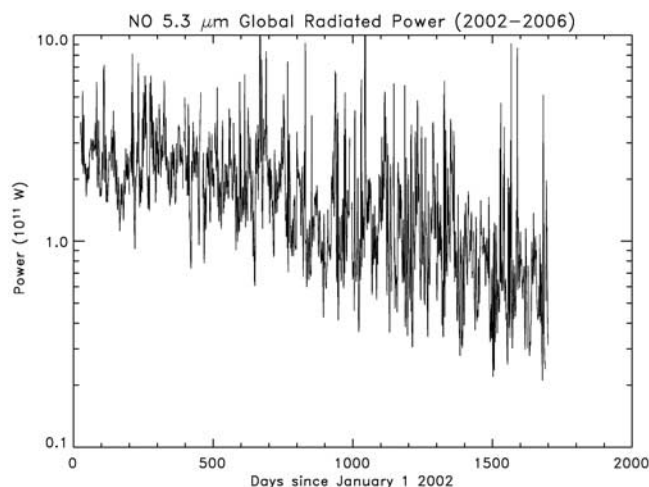


Figure 2. Time series of daily global NO power from 2002 to 2006 on a logarithmic scale.

converted to heat, the resultant heating rates are locally very small in the lower atmosphere.

[8] The altitude range of the vertical integration is 100 km to 200 km. Our studies have shown that the emission above 200 km adds on only several percent to the total global power. The derived fluxes are sorted into 5-degree bins of latitude, from which the power emitted within each latitude bin is obtained by multiplying the zonal mean flux within each bin by the area of the bin. This yields the power (W) radiated every 5 degrees in latitude. The next-to-final step in the process is to add up the power from each 5-degree latitude bin to obtain the total power radiated by the NO molecule. We note that *Mlynchak et al.* [2005] incorrectly applied a cosine latitude weighting factor to the power as a function of latitude, thus underestimating the total global emitted power. This has been corrected [*Mlynchak et al.*, 2007] and the power calculations in this current paper are computed properly.

[9] The last step in the process is to recognize that owing to the SABER viewing geometry on the TIMED spacecraft, the range of latitudes observed covers from 83 degrees in one hemisphere to 55 degrees in the other. This range encompasses approximately 91% of the global atmospheric area; however, it does leave out one of the polar regions. Every 60 days the TIMED spacecraft yaws 180 degrees, enabling SABER to change its hemispherical latitude coverage. To estimate the total power radiated by the entire atmosphere (pole to pole), we assume that the ratio of the power emitted between the equator and 55 degrees latitude to the power emitted from 55 degrees to the pole is the same in both hemispheres. This provides an estimate of the power emitted by the entire atmosphere.

3. Results

[10] The process above was followed by *Mlynchak et al.* [2005] to analyze the ten days in April 2002 during which a very strong geomagnetic disturbance occurred accompanied by a large increase in the strength of the NO emission from the thermosphere. This process is now applied to the entire SABER data set. Shown in Figure 1 are five frames of data

showing the daily global power radiated by NO from 2002 (when routine mission operations began) through August 2006. The feature that is most readily apparent in the data is the variability of the daily NO power. Also readily apparent are the major storm events such as the “Halloween Superstorms” shortly after day 300 in 2003, and again after day 310 in 2004, when the daily global power emitted by NO exceeded 1 terawatt. The events studied in detail by *Mlynchak et al.* [2005] correspond to the enhanced power at day 110 in 2002. Upon closer inspection of the data in Figure 1 it is clear that the overall level of radiated power by NO has decreased from 2002 to 2006. To more clearly illustrate the overall temporal variation and decrease of the daily power we plot in Figure 2 on a logarithmic scale the data from Figure 1 as one continuous time series. It is evident that the NO power has been steadily decreasing since the start of the mission, although the signal is highly variable.

[11] We will begin to assess and quantify the magnitude of the decrease in NO power by examining the time series presented in Figure 2 and computing the Lomb-normalized periodogram, which we show in Figure 3. The advantage of the Lomb periodogram is that it allows the significance of various features in the power spectrum to be assessed. In Figure 3 we have indicated the 95% and 50% significance levels. The largest peak power is observed to occur with a period of 60 days, the yaw period of the TIMED spacecraft. There are also significant peaks with periods of 210 and 9 days. Although not shown, these peaks also occur in a traditional Fourier transform of the data, confirming the Lomb calculations.

[12] Owing to the variability of the NO data, and the recurring 60-day feature due to the yaw cycle, we will need to smooth the time series by computing running means, in order to derive a meaningful measure of the decrease in the NO power with time. We first examined 27- and 60-day running means. These did not eliminate the 60-day feature, but in fact made it more obvious by the reduction of finer-scale variability. We decided finally

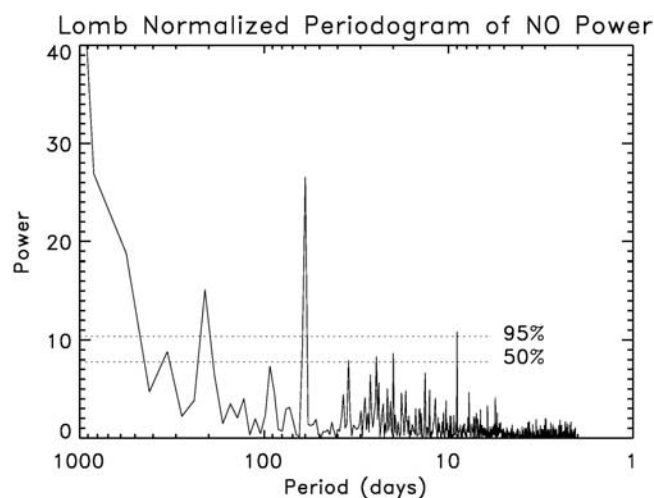


Figure 3. Lomb-normalized periodogram of the NO power time series in Figure 2. The 95% and 50% significance levels are indicated by the horizontal dotted lines.

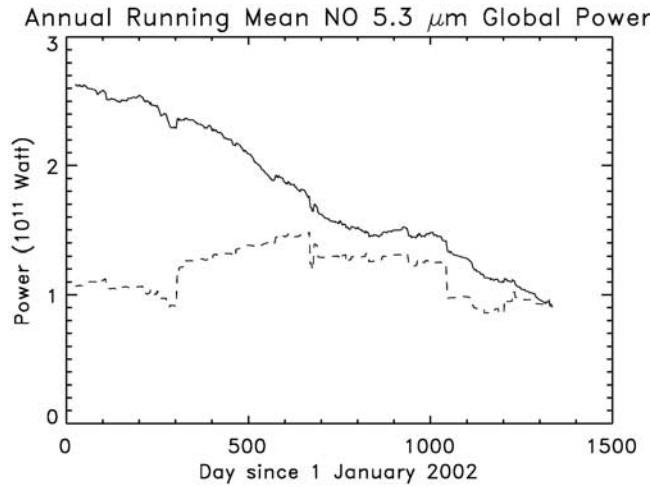


Figure 4. Running annual mean of the daily global NO power from Figure 2 (solid curve) and the corresponding standard deviation of the running mean (dashed curve).

upon a 365-day (i.e., annual) running mean, which fully eliminated the 60-day variability and which likely provides a more appropriate measure of the thermospheric long-term variability or “climate.”

[13] Starting at day 25 in 2002 (the first fully operational day for SABER), we compute the running mean for the next 365 days of data. We do this again for day 26, and so on for each consecutive day, obtaining over 1300 values of the annual running mean. Days in which there is little or no SABER data are not included; typically this is no more than five to eight days in any 365 day window. We note that the period of one year also corresponds to an integral number of spacecraft yaw cycles, six in the case of the TIMED satellite.

[14] In Figure 4 we show with the solid curve the running annual mean computed from the start of the mission. The abscissa indicates the first day of the 365 for which the mean is computed. In this sense the means can be interpreted as “forward” running means starting from the indicated day. The dashed curve in this figure is the standard deviation of the annual means, again in the “forward” sense. Clearly evident is a decrease in the NO power from the start of the mission, by a factor of approximately 2.9. Despite this large decrease, the standard deviation remains essentially constant over this time. The observed increase in the standard deviation at day 300 is a direct consequence of the forward running mean now including the “Halloween superstorm” of October 2003. Similarly, the decrease in the standard deviation after day 1000 is a consequence of the running mean no longer including the terawatt event near day 315 in 2004 (see Figure 1).

[15] The observed decrease in the NO power occurs during the declining phase of the present solar cycle. Over the same time period covered in Figure 4, the annual running mean F10.7 index decreases monotonically from 175 to 83. Shown in Figure 5 is a plot of the running annual mean NO power derived from SABER measurements against the running annual mean F10.7 solar index. The linear correlation coefficient for these data is 0.96. The solid

curve in Figure 5 represents a second-order polynomial fit to the data. Specifically,

$$P = a_0 + a_1 F + a_2 F^2, \quad (1)$$

where P is the annual running mean of NO power (10^{11} W, forward one year), F is the annual running mean F10.7 index (again, forward one year from a given date), and a_0 , a_1 , and a_2 are equal to -3.85 , 7.51×10^{-2} , and -2.18×10^{-4} , respectively. Equation 1 provides a fundamental relationship between solar variability and the dominant term in the infrared energy balance of the entire thermosphere. It also provides a fundamental empirical constraint that can be used in testing numerical models of the thermosphere, in the sense that the annual power computed in a model run of one year or longer can be compared with the F10.7 index values which are often used to parameterize the solar variability in the models.

4. Analysis

[16] To understand the reasons for the variability in the NO radiated power, it is instructive to consider the expression for the flux (F , W m^{-2}) radiated by NO at a specific latitude and longitude. Recall that the volume emission rate derived by SABER is the volume emission rate (W m^{-3}) of energy which is directly related to the radiative cooling rate through the first law of thermodynamics. Specifically, we can write (to first order) from the definition of the flux and the first law:

$$F = \int_z V(z) dz = \int_z \rho(z) C_p \frac{\partial T(z)}{\partial t} dz, \quad (2)$$

where $V(z)$ is the SABER-derived volume emission rate, $\rho(z)$ is the density, C_p is the heat capacity at constant pressure, and $\partial T(z)/\partial t$ is the rate of radiative cooling (K day^{-1}). Thus the flux, and hence the global power

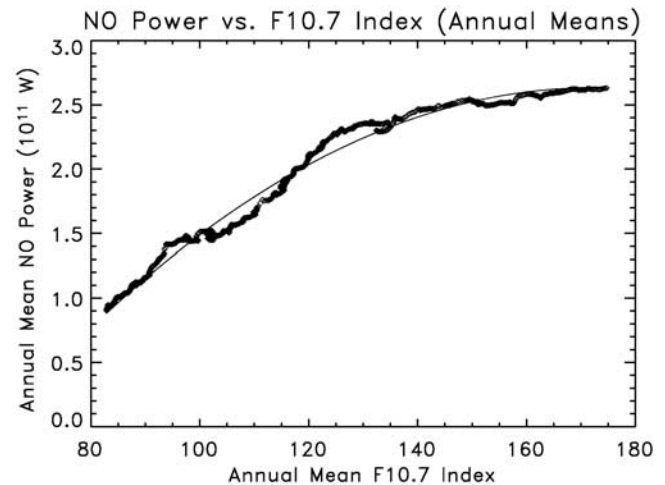


Figure 5. Running annual mean of the global NO power plotted against the running mean of the F10.7 solar index. The smooth curve is the equation fit to the data described by equation (2).

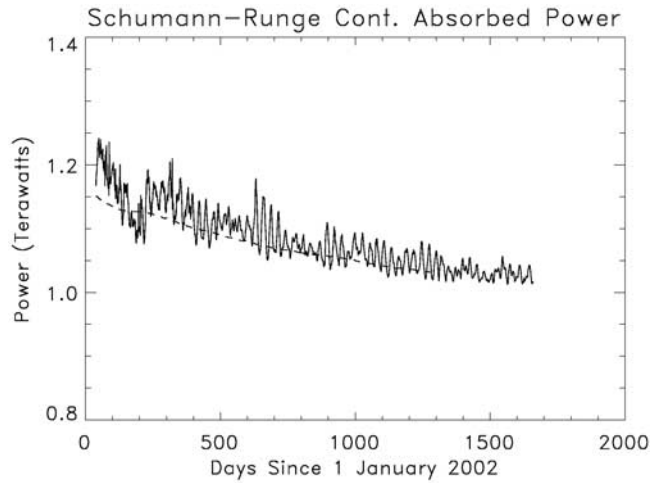


Figure 6. Absorbed power (Terawatts) in the Schumann-Runge Continuum based on Solar EUV Experiment and Solar Radiation and Climate Experiment data. Daily power is indicated by the solid curve, and the annual mean power is in the dashed curve.

presented above, represents the density-weighted, vertically integrated radiative cooling rate of the thermosphere. The observed decrease in the flux and power radiated by NO directly implies a decrease in the radiative cooling of the thermosphere that is coincident with the decline in activity in the current solar cycle.

[17] To further interpret the observed decrease in radiated power, to first order we can write the flux F as:

$$F = E_{10} A_{10} k_{10} g_0 \int_z \frac{[NO(z)]}{Q(z)} [O(z)] \frac{\exp[-E_{10}/k_B T(z)]}{A_{10} + k_{10}[O(z)]} dz. \quad (3)$$

Equation (3) is derived from a vertical integration of the volume emission rate, assuming a two vibrational level NO molecule, i.e., a ground state and a first excited state for NO. Only spontaneous emission of radiation from the first excited state and collisional excitation and quenching (by collisions with atomic oxygen) of ground and excited state are considered for this illustration. In equation (3) $NO(z)$ and $O(z)$ are the concentrations of nitric oxide and atomic oxygen at altitude z , respectively, A_{10} is the lifetime against spontaneous emission of the first excited NO vibrational level, k_{10} is the rate coefficient for quenching of the first excited state of NO in collisions with atomic oxygen, E_{10} is the energy of the first excited state above ground, k_B is Boltzmann's constant, $Q(z)$ is the vibrational partition function for NO, g_0 is the degeneracy of the ground state, and $T(z)$ is the kinetic temperature at altitude z . We note that k_{10} , being independent of temperature [Hwang *et al.*, 2003], is effectively constant with altitude.

[18] Upon inspection of equation (3) it is evident that the flux (and hence the radiated power) depends linearly on the NO density, at most linearly on the atomic oxygen density, and nonlinearly on temperature. We would expect all three quantities (NO, O, and T) to decrease during the declining phase of a solar cycle because less ultraviolet radiation enters the thermosphere from the Sun. The extent to which

the relative variability of these three factors individually influences the variability of the radiated power remains to be quantitatively determined.

[19] Some insight is gained into the importance of the variability of the NO density by examining the correlation between the NO power and the NO column density, the latter as observed by the HALOE instrument (from the lower stratosphere into the lower thermosphere) that operated on the UARS satellite through 2005. Owing to sampling issues, the latitude range of the HALOE data for this purpose is ± 45 deg. Within these parameters, there are about 490 days in which both HALOE and SABER were operational before the UARS mission was ended in 2005. The linear correlation coefficient between the lower thermospheric (105 to 140 km) column NO derived from HALOE and the power derived from SABER is found to be 0.59, when taking the NO power between ± 55 degrees latitude, the latitude range continuously observed by SABER. The relatively low correlation coefficient, for these latitudes at least, suggests that variations in NO density alone are not adequate to account for the observed variations in NO infrared radiated power.

5. Consistency With Changes in Solar Energy Output

[20] From the annual mean NO power presented above we can compute the change in the outgoing longwave radiation from the thermosphere from the start of the TIMED mission. Using the data presented above, the change in the running annual mean power from day 39 2002 until day 199 2005 is found to be 1.65×10^{11} W (165 GW). We can compare this with the change in solar output by comparing with the change in ultraviolet radiation measured by the Solar EUV Experiment (SEE) on TIMED [Woods *et al.*, 2005] and by the Solar Radiation and Climate Experiment (SORCE) [Rottman, 2005].

[21] We first consider the change in the absorbed UV radiation in the Schumann-Runge Continuum (SRC). The cross sections in this band are independent of temperature and pressure. Thus the global absorbed power P is estimated by:

$$P = \pi r_{\text{eff}}^2 \sum_{\lambda} F_{\lambda}^o (1 - \exp(-\sigma_{\lambda} u)) \quad (4)$$

where P is the global absorbed power (W), F_{λ}^o is the exoatmospheric solar irradiance ($\text{W m}^{-2} \text{nm}^{-1}$, from SEE and SORCE), σ_{λ} is the SRC cross section (cm^2) at wavelength λ , and u is the optical mass (cm^{-2}). To estimate the global power we use an optical mass of molecular oxygen (O_2) above 100 km of $2 \times 10^{18} \text{ cm}^{-2}$ based on a vertical optical mass of $1 \times 10^{18} \text{ cm}^{-2}$ and a global mean solar zenith angle of 60 degrees. The term r_{eff} is the effective radius of the Earth's disk that absorbs the UV radiation, which we take to be 6520 km, or 150 km larger than the average Earth radius. The summation is carried out in 1 nm bins from 130.5 nm to 173.5 nm. The Lyman- α line at 121.5 nm is included in addition to the SRC and adds a few percent to the sum.

[22] SORCE was launched in early 2003 and data are available from 25 January 2003. In comparisons with the

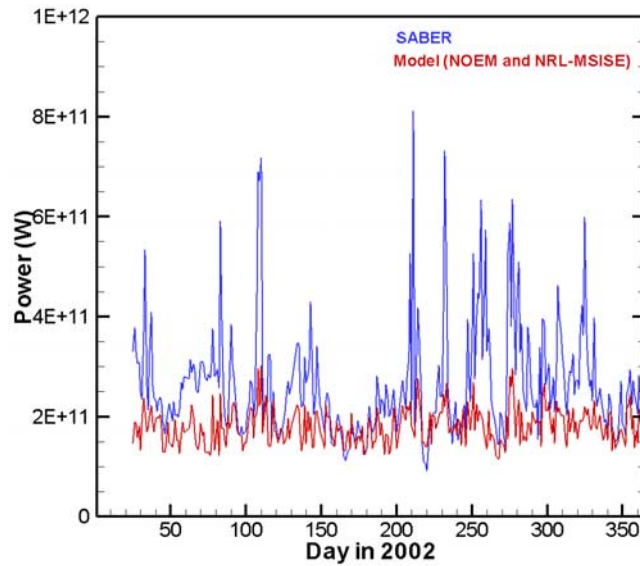


Figure 7a. Daily global power from NO as measured by Sounding of the Atmosphere using Broadband Emission Radiometry (SABER) (in blue) and as computed from the nitric oxide empirical model (NOEM) of *Marsh et al.* [2004] for the year 2002.

SEE data an offset between the two data sets of about 8% was observed, with the SEE SRC being larger. To construct a continuous solar irradiance data set from the start of the TIMED mission we combine SEE data (scaled down by a factor of 1.08) from January 2002 until January 2003, and then use SORCE data from that point forward. The SORCE data are believed to be more accurate than the SEE data at this point in time.

[23] Using this blended set of solar irradiance data, we compute P as defined above for each day and then evaluate the annual running mean in the same way as for the NO power from SABER. Although the archived SEE and SORCE data are nominally at 1 AU, we have adjusted them to reflect the actual Earth–Sun distance. Shown in Figure 6 is the daily absorbed power (solid curve) estimated according to equation (4) and the corresponding daily running mean power (dashed curve). The correlation between the decrease in the annual mean NO power and the annual mean power absorbed in the Schumann-Runge continuum is 0.98.

[24] From these data we determine that the change in absorbed UV in the SRC over the same extent of time as the SABER NO data is 2.05×10^{11} W or 205 GW. The majority of the absorbed energy in the SRC in fact goes into chemical potential energy of atomic oxygen which is realized as heat only long after the time of photon deposition, as the O is transported downward to an altitude where density is sufficient for recombination to occur. Thus the difference between the NO power and the SRC is perhaps not surprising – the majority of the energy absorbed in the SRC is likely not liberated in the thermosphere.

[25] There are of course several other important terms in the energy budget of the thermosphere. All solar radiation shorter than 120 nm is absorbed in the thermosphere, and Joule and particle heating are important. *Knipp et al.* [2005]

note changes of 203 GW in solar radiation below 120 nm and 35 GW in Joule heating from solar maximum to solar minimum. Cooling due to emission from CO₂ at 15 μ m and atomic oxygen at 63 μ m must also be considered in any detailed assessment of the overall energy budget, and will be the subject of a subsequent paper. Nevertheless, the change in NO emission over the course of the TIMED mission to date appears to be consistent with the changes in solar radiation considering the other terms in the balance yet to be evaluated.

6. Comparison With an Empirical Model

[26] The SABER data indicate a large decrease (factor of nearly 3) in the annualized mean power emitted from the lower and middle thermosphere during the declining phase of the current solar cycle. To further investigate this, we have also compared the observed SABER results with that obtained by evaluating equation (3) above using data from the nitric oxide empirical model (NOEM) of *Marsh et al.* [2004]. Temperature and atomic oxygen abundances required for equation (3) are taken from the MSIS 2000 model [*Picone et al.*, 2002]. For k_{10} we adopt a value of 4.2×10^{-11} cm³s⁻¹ [*Hwang et al.*, 2003] and for A_{10} 12.26 s⁻¹. The NO abundances derived in the NOEM model are developed from daytime-only observations between 100 and 150 km made by the Student Nitric Oxide Explorer (SNOE) experiment from 1998 until 2000. This comparison provides a first test of the ability of models to reproduce the observed variability in the NO emission and radiative cooling.

[27] To compare with the SABER data we compute the daily NO power in the years 2002 and 2006, and the results are shown in Figures 7a and 7b, respectively. While the observed and modeled power levels are in general agree-

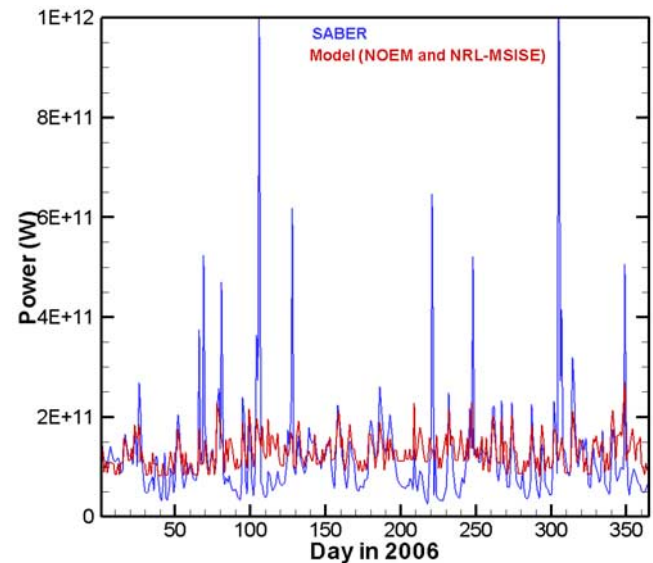


Figure 7b. Daily global power from NO as measured by Sounding of the Atmosphere using Broadband Emission Radiometry (SABER) (in blue) and as computed from the nitric oxide empirical model (NOEM) of *Marsh et al.* [2004] for the year 2006.

ment in magnitude, it is evident that the model calculations do not pick up large storm-time excursions. In addition, from visual inspection of Figures 7a and 7b, the annual average modeled power derived in 2002 is smaller than observed, while the annual average modeled power in 2006 is larger than observed. Hence the modeled change from 2002 to 2006 is not nearly as large as observed by SABER. The annualized mean modeled power decreases by 30% from 2002 to 2006, compared with the SABER-observed factor of nearly 3.

[28] The difference in the observed and modeled powers can be partly explained by the fact that the model does not cover the same range of altitudes as the SABER observations and thus does not contain all the variability. However, most of the SABER signal does come from below 150 km (the highest model altitude) so this cannot be the sole source of the discrepancy. In addition, the model is developed from a data set of NO that covers roughly one-quarter of a solar cycle as opposed to the approximately one-half of the cycle observed by SABER to date. It is plausible that the model is not able to reproduce the temporal variability in NO owing to the relatively short length of time of the data set on which it is based. Last, the actual variability in temperature and atomic oxygen may not be completely represented by the NRL MSIS model. Clearly, more detailed comparisons are warranted against models that have consistent computations of temperature and nitric oxide photochemistry.

7. Summary and Conclusions

[29] We have analyzed nearly five years of measurements of infrared emission from NO made by the SABER instrument on the TIMED satellite. SABER limb radiance measurements are inverted to yield vertical profiles of the volume emission rate of energy from the NO molecule. The emission rates are then used to derive the daily global power radiated by the NO molecule from the thermosphere between 100 and 200 km altitude. The data exhibit significant day-to-day variability. Over the period of extant data, the daily NO power is observed to decrease significantly. The observed decrease in radiated power is directly related to a decrease in the radiative cooling rate of the thermosphere. The annual running mean power decreases by a factor of 2.9, and is strongly correlated with the decrease in the annual running mean value of the F10.7 solar index, implying that the observed decrease in NO power (and the associated radiative cooling rate) is caused by the decline in solar activity. The variance of the annual means remains essentially constant and is visibly influenced by the occurrence of major storm events (e.g., those in which the daily power radiated by NO is found to exceed one terawatt.) The magnitude of the change in NO emission appears consistent with that expected from changes in solar inputs. Illustrating the complexity of the lower thermosphere, a first comparison of these observations with those derived from empirical model data indicate the models underestimate the magnitude of the variability on short and long timescales. Comparisons with more detailed and consistent models are clearly warranted.

[30] The last day of NO data used in the analysis above was day 238 of 2006. The NO power data through this date (i.e., Figures 1 and 2) do not yet exhibit evidence to confirm

that solar minimum has been reached. It is anticipated that the NO power will increase as the Sun passes through the minimum of the current 11-year cycle and begins building up to the next maximum. The database of NO power will be continually updated as the TIMED mission goes on for the next several years. The database of NO power presented here, which also includes values of the A_p , K_p , and F10.7 indexes, is available from the first author of this paper at the e-mail address given below. These data should prove valuable in studying the relative roles of natural and anthropogenic change in the thermosphere.

[31] **Acknowledgments.** The authors would like to thank the NASA Science Mission Directorate for continued support of the TIMED mission and the SABER project. MGM would like to thank the NASA Langley Science Directorate for continued support.

References

- Ballard, J., B. J. Kerridge, P. E. Morris, and F. W. Taylor (1993), Observations of $V = 1-0$ emission from thermospheric nitric oxide by ISAMS, *Geophys. Res. Lett.*, **20**, 1311–1314.
- Gardner, J., B. Funke, M. G. Mlynczak, M. López-Puertas, F. J. Martín-Torres, J. M. Russell III, S. M. Miller, R. D. Sharma, and J. R. Winick (2007), Comparison of nighttime nitric oxide $5.3 \mu\text{m}$ emissions in the thermosphere measured by MIPAS and SABER, *J. Geophys. Res.*, **112**, A10301, doi:10.1029/2006JA011984.
- Hwang, E. S., K. J. Castle, and J. A. Dodd (2003), Vibrational relaxation of NO ($v = 1$) by oxygen atoms between 295 and 825 K, *J. Geophys. Res.*, **108**(A3), 1109, doi:10.1029/2002JA009688.
- Knipp, D. J., W. K. Tobiska, and B. A. Emery (2005), Direct and indirect thermospheric heating sources for solar cycles 21–23, *Sol. Phys.*, **224**, 495–505, doi:10.1007/s11207-005-6393-4.
- Kockarts, G. (1980), Nitric oxide cooling in the terrestrial thermosphere, *Geophys. Res. Lett.*, **7**, 137–140.
- Marsh, D. R., S. C. Solomon, and A. E. Reynolds (2004), Empirical model of nitric oxide in the lower thermosphere, *J. Geophys. Res.*, **109**, A07301, doi:10.1029/2003JA010199.
- Mlynczak, M., et al. (2003), The natural thermostat of nitric oxide emission at $5.3 \mu\text{m}$ in the thermosphere observed during the solar storms of April 2002, *Geophys. Res. Lett.*, **30**(21), 2100, doi:10.1029/2003GL017693.
- Mlynczak, M. G., et al. (2005), Energy transport in the thermosphere during the solar storms of April 2002, *J. Geophys. Res.*, **110**, A12S25, doi:10.1029/2005JA011141. (Correction, *J. Geophys. Res.*, **112**, A02303, doi:10.1029/2006JA012008.)
- Mlynczak, M. G., F. J. Martín-Torres, and J. M. Russell III (2007), Correction to “Energy transport in the thermosphere during the solar storms of April 2002,” *J. Geophys. Res.*, **112**, A02303, doi:10.1029/2006JA012008.
- Picone, J. M., A. E. Hedin, D. P. Drob, and A. C. Aikin (2002), NRLMSISE-00 empirical model of the atmosphere: Statistical comparisons and scientific issues, *J. Geophys. Res.*, **107**(A12), 1468, doi:10.1029/2002JA009430.
- Rottman, G. (2005), The SORCE Mission, *Sol. Phys.*, **230**, 7–25, doi:10.1007/s11207-005-8112-6.
- Woods, T. N., F. G. Eparvier, S. M. Bailey, P. C. Chamberlin, J. Lean, G. J. Rottman, S. C. Solomon, W. K. Tobiska, and D. L. Woodraska (2005), Solar EUV Experiment (SEE): Mission overview and first results, *J. Geophys. Res.*, **110**, A01312, doi:10.1029/2004JA010765.
- L. L. Gordley, B. T. Marshall, and R. E. Thompson, G&A Technical Software, 11864 Canon Blvd., Suite 101, Newport News, VA 23606, USA.
- D. P. Kratz and M. G. Mlynczak, NASA Langley Research Center, Mail Stop 420, Hampton, VA 23681-2199, USA. (m.g.mlynczak@nasa.gov)
- F. J. Martín-Torres, Analytic Services & Materials, Inc., 107 Research Drive, Hampton, VA 23666-1340, USA.
- J. M. Russell III, Center for Atmospheric Sciences, 23 Tyler Street, Hampton University, Hampton, VA 23668, USA.
- T. Turpin and J. Williams, Department of Electrical and Computer Engineering, Utah State University, 4120 Old Main Hill, Logan, UT 84322-4120, USA.
- T. Woods, Laboratory for Atmospheric and Space Physics, 1234 Innovation Drive, Boulder, CO 80303-7814, USA.